AIAA JOURNAL
Vol. 36, No. 6, June 1998

Behavior of Composite Shells Under Transverse Impact and Quasi-Static Loading

Brian L. Wardle* and Paul A. Lagace†
Massachusetts Institute of Technology, Cambridge, Massachusetts 02139

The impact and quasi-static response of various composite shell structures to transverse loading was studied experimentally. In particular, the effect of varying structural parameters (radius, span, and thickness) on the loading response, including damage resistance, is explored. The AS4/3501-6 graphite/epoxy composite structures considered have a $[\pm 45_n/0_n]_s$ layup configuration ($n = 1, 2, 3$) and include convex and concave shell sections, plates, and full cylinders. All structural parameters are found to affect the response, particularly characteristics of the instability associated with the convex shell behavior and the structural stiffness. Trends with regard to peak force and structural stiffness with the structural parameters are established and discussed. Specimen thickness is noted to have the greatest effect of all the parameters, but shell radius is clearly important due to the instability that it introduces. Damage resistance trends with structural parameters are established and linked to peak force. Although linked to peak force, these damage trends are also found to be dependent upon whether the peak force occurs before or after the shell instability. The results of this work establish the effects of structural parameters on the general response characteristics, including damage resistance, of composite shells under transverse loading with application to low-velocity impact. Thus, these results provide benchmark data for comparison with analytical and numerical, e.g., finite element, studies. Suggestions for areas of further work are provided.

Introduction

LAMINATED composites continue to see increased use in high-performance, weight-critical applications, e.g., the hydrogen fuel tank in next-generation reusable launch vehicles.[1] The use is due to factors such as the high specific stiffness, excellent fatigue characteristics, and environmental properties, e.g., high operating temperatures, of these materials. However, damage resistance and tolerance of such composite structures are of significant concern due to their relatively low through-thickness strength and susceptibility to damaging events, e.g., impact. Impacted composite structures are known to have static strength reductions of 50–75% as compared with undamaged specimens.[2–4] Reviews of the current literature show that although the impact response of composite plates has been studied rather extensively, very little work exists concerning composite shell structures.[4–6] This is unfortunate because real aerospace structures such as wings and fuselages are most accurately characterized as shells, not plates.

Prediction of the structural response of composite shells requires significant computational effort due to factors such as nonlinear geometric (kinematic) couplings, large rotations, and buckling of the structure. Issues such as these preclude the use of simplified classical arch analyses to determine structural response. Alternatively, numerical studies, particularly finite element analyses, have been used to characterize the structural response of (composite) shells to static transverse loading, e.g., Refs. 7–11, and also to impact, e.g., Ref. 7. For the case of square planform hinged shells of the type considered herein, these analyses have all relied solely on comparison to other analyses for validation purposes; no experimental data exist for comparison and verification. Experiments also incorporate aspects of the response that are difficult, if not impossible, to otherwise identify (through analyses). These aspects include response asymmetries, imperfection sensitivity, boundary condition specifics, and loading misalignments—everything an analysis of a real structure demands. Factors such as these, and therefore their importance, can only be modeled once they have been identified. Thus, although modeling techniques exist, there remains a lack of experimental data for comparison and insight. A need exists to experimentally characterize the response of composite shells to such transverse loading.

The present work was undertaken in a general sense to experimentally characterize and explore the response of composite structures with a wide range of structural configurations to both impact and quasi-static loading. Given classical definitions of deepness based on arch-type analyses, e.g., Ref. 12, the resulting structures range from shallow to deep shells. The impacts events are of interest due to real (in-service) damaging events such as tool drop and bird strike. The effects of varying structural parameters (radius, span, and thickness) on the resulting response (including damage) are particularly addressed in this work.

Approach

Impact and quasi-static testing were undertaken to determine the response, including damage, of a wide range of composite structures to transverse, centered loading. Singly curved composite shell structures were manufactured from Hercules AS4/3501-6 prepreg tape in a $[\pm 45_n/0_n]_s$ configuration, where $n = 1, 2$, and 3. The composite structures are singly curved shells having square planform and include convex and concave shell sections, plates, i.e., shells with a radius of ∞), and cylinders. The orientation of the ply angle (θ) with respect to specimen curvature in shown in Fig. 1. The shells are restrained in a specially designed test fixture with boundary conditions of pinned/no in-plane sliding (hinged) on the circumferential edges and free on the axial edges (edges defined in Fig. 1).

As this work is an exploratory investigation, specimen structural parameters were varied to give a wide range of geometrical characteristics. Radius, span, and thickness were independently varied via scaling considerations. Scaling of the structural parameters is based on effective ply thickness, the total thickness of adjacent plies with the same fiber orientation. As the number of ply interfaces (between plies at different orientations) changes, delamination extent and through-thickness distribution change, thereby affecting the mix of different damage mechanisms.[13] This issue was avoided by utilizing effective plies to keep the number of ply interfaces constant despite different specimen thicknesses. Thus, changes in damage mode and extent were isolated to effects from structural parameters on the resulting response. Using effective plies as the basis for

Received Feb. 5, 1997; presented as Paper 97-1059 at the AIAA/ASME/ASCE/AHS/ASC 38th Structures, Structural Dynamics, and Materials Conference, Kissimmee, FL, April 7–10, 1997; revision received July 11, 1997; accepted for publication Dec. 30, 1997.

*Ph.D. Candidate, Technology Laboratory for Advanced Composites, Department of Aeronautics and Astronautics. Student Member AIAA.

†Professor and MacVicar Faculty Fellow, Technology Laboratory for Advanced Composites, Department of Aeronautics and Astronautics. Associate Fellow AIAA.

Table 1 Nominal structural parameters

n	R_n = radius, mm	S_n = span, mm	T_n = thickness, mm
1[a]	152	102	0.804
2	305	203	1.608
3	457	305	2.412

[a]Base values have n equal to 1.

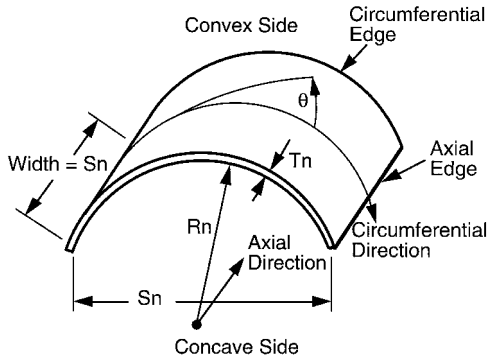

Fig. 1 Illustration of generic test specimen showing radius, span, thickness, and ply angle.

scaling, three different values for each of the structural variables are obtained via

$$X_n = n(X_1) \tag{1}$$

where X represents any of the three structural parameters, X_1 represents the base value for structural parameter X, and n takes on the values 1, 2, and 3. Base values and the resulting structural parameters are given in Table 1. The specimens are noted to range from very shallow to extremely deep (half-cylinder) shells. Intermediate values of span and thickness, i.e., S_2 and T_2, approximately correspond to values for stringer spacing (span) and thickness for a typical commercial aircraft.[14] Thus, the loadings (e.g., impact) considered herein are representative of a transverse impact event to a composite fuselage section.

Impact velocities of 1, 2, 3, and 4 m/s were found to provide specimen responses ranging from purely elastic (no damage) to severe damage (specimen penetration) during preliminary testing. This range of response was deemed desirable from a damage resistance/tolerance perspective and was therefore chosen for the test matrix. It was also found from preliminary tests that an impact velocity of 3 m/s would damage the majority of specimens in this investigation. Therefore, quasi-static testing was conducted until the maximum load measured during an impact test at 3 m/s of a concomitant specimen was reached so that damage states from the two test types could be compared based on the damage resistance metric of peak force.[15,16]

Structural scaling considerations along with the findings from preliminary testing were used to construct the test matrix presented in Table 2. The test matrix contains 94 specimens but is not fully populated. Attention was paid to the distribution of unpopulated entries in the test matrix so that information from testing could be used to establish trends that encompass unpopulated regions.

During each impact test, the impactor force-time history was measured to determine the specimen response. Force-deflection histories were measured to characterize the response in the quasi-static tests. All specimens were visually evaluated for damage after testing and the dye-penetrant-enhanced x-radiography method was utilized to determine the extent and distribution of nonvisible damage.

Experimental Specifics

Detailed information on the experimental procedures given here can be found in Ref. 17. Specimen preparation and setup for the impact and quasi-static tests were identical.

Specimen Preparation

Shells were manufactured using standard layup and cure procedures for this material system[18] except that the laminates were cured on specially designed cylindrical molds. Full cylinders were cured on a 305-mm (12-in.) diameter mandrel. Laminates were layed up by hand and processed using the standard manufacturer's cure cycle of a 1-h flow stage at 116°C and a 2-h set stage at 177°C. This was conducted in an autoclave under vacuum with 0.59-MPa external pressure. Laminates were postcured in an oven at 177°C for 8 h and subsequently cut to the desired dimensions using a water-cooled diamond-grit cutting wheel.

Specifics of the manufacturing procedure can be found in Ref. 17, including an evaluation of the manufacturing technique, which shows that the specimen quality is typical of standard plate specimens. Average specimen thicknesses (and radii) are all within 4% of the nominal values with acceptable coefficients of variation (less than 3% for thickness and 5% for radii).

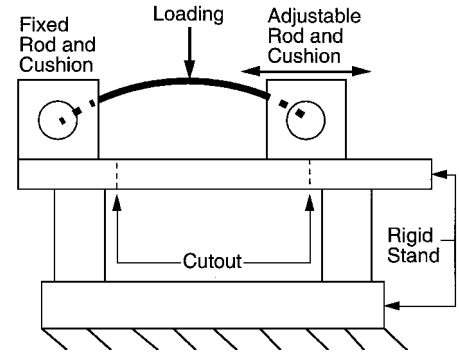

Fig. 2 Side-view illustration of test fixture with convex shell. Note: not to scale.

Test Fixture

The shells (and plates) were restrained in a specially designed test fixture with boundary conditions of pinned/no in-plane sliding (hinged) on the axial edges and free on the circumferential edges (edges defined in Fig. 1). Fixing the in-plane boundary condition exaggerates compressive membrane (in-plane) stresses developed in the initial loading of the convex shells, which is a basic (structural response) difference between convex shells and plates. An overall view of the test fixture is presented in Fig. 2 for a convex shell. The test fixture consists of two primary components for restraining specimens along the axial edges: adjustable rods and cushions in which the rods rest. Shells are restrained out of plane using steel knife edges, which actually have a 1.59-mm (1/16-in.) radius, that support the shell along the entire axial edge. The in-plane restraint is accomplished by the shell impinging on the flat face of the rod. Plates and concave shells require additional consideration (and attachments) because the in-plane condition at the boundary is tensile (pull out), whereas for convex shells it is compressive (push in) before the instability. The no-sliding in-plane condition for these cases is attained by bolting extended knife edges to the axial plate (or shell) edges. The knife-edge ends of these attachments rotate about a point coincident with the hinged boundary condition thereby allowing rotation but prohibiting in-plane motion. A detailed description and performance evaluation of the test fixture, found in Ref. 17, shows that the test fixture allows rotation at the pinned boundaries and adequately restrains the specimens (plates, concave, and convex shells) as desired.

Full cylinders are supported at three locations (in cross section) as shown in Fig. 3: at the floor (bottom of cylinder) and at two angle irons spaced 254 mm apart (symmetric about the cylinder bottom) and 57.2 mm above the floor. This configuration allows elongation of the cylinder diameter perpendicular to the loading direction.

Impact Testing

A device previously developed for impact testing of composite structures[19] was used to horizontally accelerate a steel impacting rod (total mass of 1.60 kg) mounted in linear bearings to the desired velocities. A light-gate assembly is used to measure the impactor velocity (within ±0.1 m/s) just before specimen contact. A force transducer, mounted behind a 12.7-mm (1/2-in.) diameter

Table 2 Test matrix

	T_1				T_2				T_3			
Span	R_1	R_2	R_3	R_P[a]	R_1	R_2	R_3	R_P	R_1	R_2	R_3	R_P
S_1	4[c]	4	4	4	1	4	1	1	1	1	4	1
S_2	4	1	1	——	——	1	——	——	——	1	1	——
S_3	4	1	1	——	——	1	1	——	——	——	1	——
S_1 concave	4	1	1	——	1	1	——	——	1	——	1	——
S_C[b]	4	——	——	——	——	——	——	——	——	——	——	——

[a] R_P indicates plate configuration (radius equal to ∞).
[b] S_C indicates full cylinder.
[c] Indicates one quasi-static test and number of impact tests at different velocities.

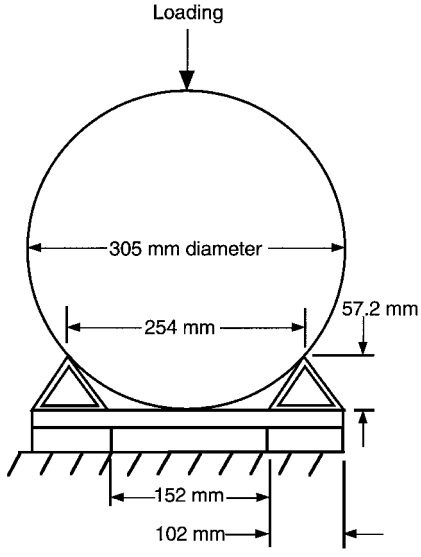

Fig. 3 Illustration of boundary condition for full cylinders. Note: not to scale.

hemispherical steel tup on the impacting rod, measures load within ±4.2 N (0.95 lb).

Because of the dynamic nature of the impact, the force measured by the transducer must be modified to account for the inertia of the tup.[20] In this investigation, the force on the tup (specimen) is 1.09 times the force measured by the transducer. Voltage output from the force transducer is digitized using a MacADIOS II analog/digital converter and recorded on a Macintosh IIx computer at 50 kHz. The measured force-time data can be twice integrated to give deflection-time data:

$$w(t) = \int_0^t \left[\int_0^t a(t)\,\mathrm{d}t + v_0 \right] \mathrm{d}t + x_0 \qquad (2)$$

where $w(t)$ is deflection, $a(t)$ is the modified (to account for the tup inertia) force-time history divided by the mass of the impacting assembly, t is time, v_0 is the measured initial velocity, and x_0 is the initial specimen deflection, which is zero. The integrations are performed using the trapezoidal rule where the time step is equal to the data-sampling interval of 20 μs.

Quasi-Static Testing

Quasi-static testing was performed with an MTS-810 uniaxial testing machine under stroke (deflection) control. An MTS 8896-N (2000-lb) load cell is used to measure the force on the specimen, and the stroke of the testing machine is used to measure deflection. Force resolution for quasi-static testing is 0.9 N (0.2 lb), whereas the deflection resolution varies with stroke range but is always better than ±0.06 mm. Peak force is known a priori for each test from the impact tests at 3 m/s, and peak deflection is estimated using Eq. (2) to obtain an approximate stroke range for each test. The stroke rate is set so that loading and unloading each lasts 3 min, giving a total test time of 6 min for each specimen. Data are sampled at 2 Hz with the same data acquisition system previously described. Although the data are not reported herein, indentation of the specimens was also measured using a linearly variable differential transformer displacement transducer placed directly under the indentor.

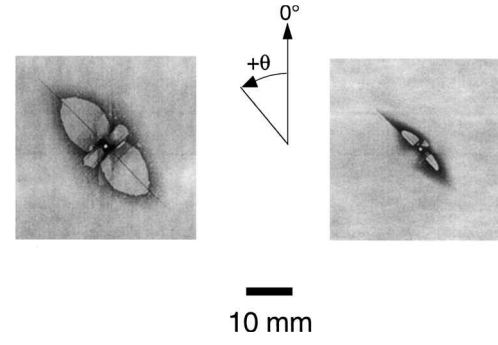

Fig. 4 Typical x radiographs of damage: shown are specimen types (on the left) $R_1S_1T_3$ (concave) impacted at 3.0 m/s and (on the right) $R_PS_1T_1$ (plate) impacted at 2.1 m/s.

Damage Evaluation

Dye-penetrant-enhanced x radiography[21,22] and visual inspection were used to characterize damage.[17] Dye penetrant was injected via a syringe into a 0.79-mm-diam hole drilled through the damage area. Flash tape was placed on the back surface of the specimens to contain the dye. This technique allows an integrated view (through the thickness) of delamination and matrix cracking. Typically, the dominant delaminations and matrix cracks extend in the +45- and −45-deg directions, with the +45-deg direction always having a greater extent, as shown in the sample x radiographs provided in Fig. 4. This type of damage is typical of that found in previous plate investigations, e.g., Ref. 23, where the major axis of the delaminations is generally parallel to the fiber direction of the lower ply. Two damage metrics were defined for use with the planar x-radiograph view of the damaged specimen. The delamination lengths in the +45- and −45-deg directions were measured to the nearest millimeter and then averaged to yield an average damage extent metric. The ratio of delamination length in the −45-deg direction to that in the +45-deg direction yields a damage extent ratio that is used to quantify the distribution of damage. The average damage extent and damage extent ratio for the two specimens shown in Fig. 4 are, respectively, 20 mm and 0.44 ($R_1S_1T_3$ concave) and 8 mm and 0.33 ($R_PS_1T_1$).

Results and Discussion

In considering the results of this work, there are three items that are important to note up front. The first is a snap-through-type instability evident in the loading response of many of the convex configurations. This type of instability has been studied extensively in the literature for arches (a summary can be found in Ref. 24) and shells, e.g., Refs. 12 and 25. In these cases, as illustrated using quasi-static data in Fig. 5, the loading progresses along the first equilibrium path until a critical load is reached (oftentimes referred to as the buckling load or herein as the critical snapping load). After the critical snapping load, the response follows a stable path through an instability region to the second equilibrium path. As with arches (and line-loaded shells), the first equilibrium path is associated with compressive membrane stresses (in the circumferential direction in Fig. 1), whereas tensile membrane stresses develop along the second. Thus,

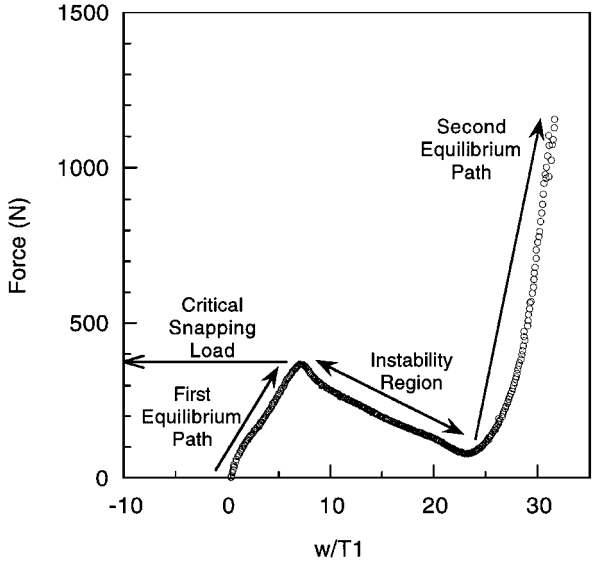

Fig. 5 Illustration of definitions used to describe instability characteristics: force vs normalized deflection data from quasi-static test of convex specimen $R_1S_1T_1$.

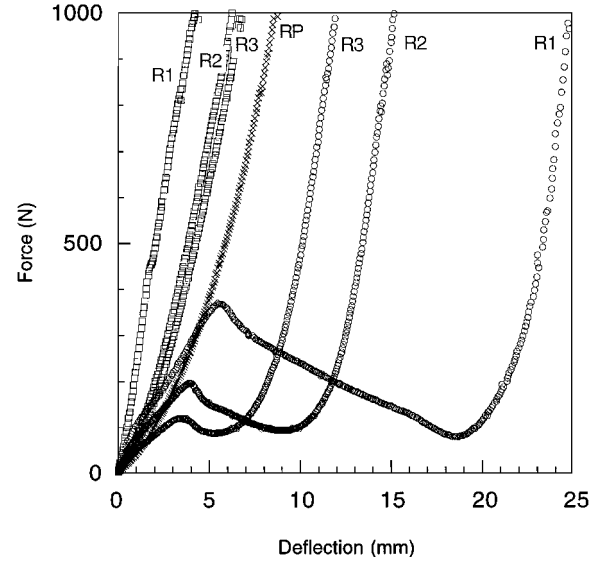

Fig. 6 Quasi-static loading response of S_1T_1 concave, plate, and shell specimens: □, concave; ×, plate; and ∘, convex.

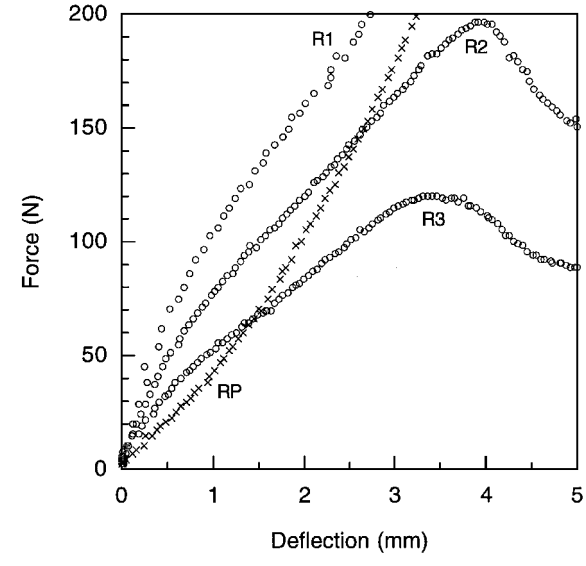

Fig. 7 Blowup of Fig. 6: quasi-static loading response of S_1T_1 plate specimen and convex shell specimens of various radii: ∘, convex, and ×, plate.

the sign of the circumferential membrane stress switches in the transition between equilibrium paths. The large-deflection behavior of the instability is illustrated by nondimensionalizing the deflections with respect to specimen thickness in Fig. 5. The presence of the instability in many convex shell responses results in differences in many of the response characteristics, including peak impact force, damage extent, and damage distribution. Thus, results must be considered within the context of the instability.

The second item to note is the equivalence of quasi-static and impact tests in this regime, which has previously been established.[17,26] Thus, in regard to studying the effects of varying structural parameters on the resulting response of the structures in this investigation, quasi-static data are used interchangeably with impact data. Therefore, quasi-static data are utilized in this paper to elucidate the effects of the structural parameters, and the conclusions are directly applicable to the impact tests due to the response equivalence.

The third item is the importance of peak force as the controlling damage resistance metric. In impact and quasi-static testing of the same structure, the resulting damage state is correlated to peak force, and furthermore, damage is shown to increase with peak force.[17,26] This is a well-known result for composite plate structures. The effect of varying structural parameters on damage resistance can therefore be evaluated by considering the effect on the resulting peak force; e.g., if increasing the radius increases the peak force, then increasing the radius will generally cause an increase in the damage. Peak force is the key to understanding damage resistance and will be considered in detail later in this section.

Effects of Structural Parameters

The structural response is characterized in two ways. First, the load-deflection response reflects the overall specimen behavior and can be particularly characterized by the initial and secant stiffnesses. As part of characterizing the load-deflection response, the critical snapping load, which indicates the onset of instability, and the deflections associated with the instability are key traits for convex specimens. Second, the peak force attained in the response (as well as the equilibrium path on which it occurs) is a measure of the impact damage resistance of the composite structures. Trends in these response characteristics were noted for each of the three structural parameters (radius, span, and thickness) considered.

The most obvious structural difference between plate and shell structures is the radius of curvature. The quasi-static load-deflection response shown in Fig. 6 for concave, plate, and convex specimens with the same span (S_1) and thickness (T_1) illustrates the effect of radius on the loading response with the instability being the most immediate effect (difference). The convex shell results in Fig. 6 clearly show that as the radius increases, both the critical snapping load and the deflections associated with the instability decrease. This behavior is noted for all convex shells tested.

With the introduction of the instability with radius, the overall loading response for the convex shells can be compared with the other configurations. The plate behavior is noted to be the limiting response as it represents the case of increasing the radius indefinitely (radius equal to ∞ or curvature equal to zero) for both the convex and concave specimens. This response trend with radius can be further elucidated by considering trends in the load-deflection response, particularly structural stiffness trends, before and after the instability. The initial loading response for the plate and convex shell specimens in Fig. 6 are shown in Fig. 7. During the initial loading, specimens with larger radius are less stiff with the plate configuration being the least stiff, i.e., most compliant. This trend of decreasing initial stiffness with increasing radius is found for all specimens tested and is evident for concave specimens in Fig. 6 with radius considered in an absolute sense, i.e., only the magnitude and not the sign is considered. However, it can be seen in Fig. 6 that the overall specimen stiffness (secant stiffness) decreases with decreasing radius (after the instability for convex specimens), i.e., the stiffness trend reverses for convex shells with an instability. Concave specimens, however, have the same trend of decreasing initial

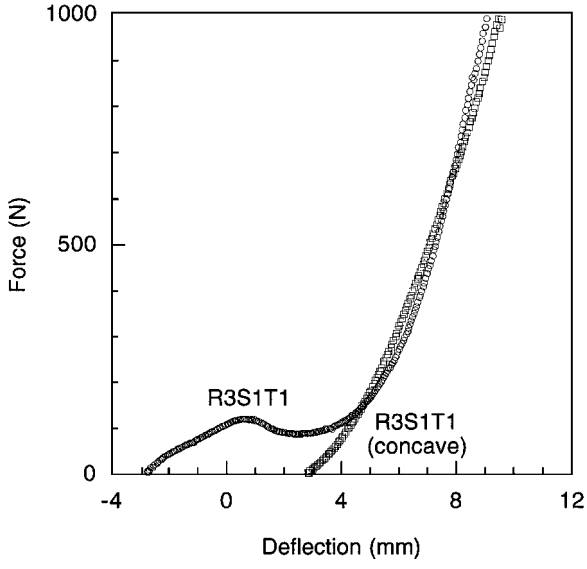

Fig. 8 Quasi-static force-deflection response with shifted deflection origin for specimen types $R_3S_1T_1$ and $R_3S_1T_1$ (concave).

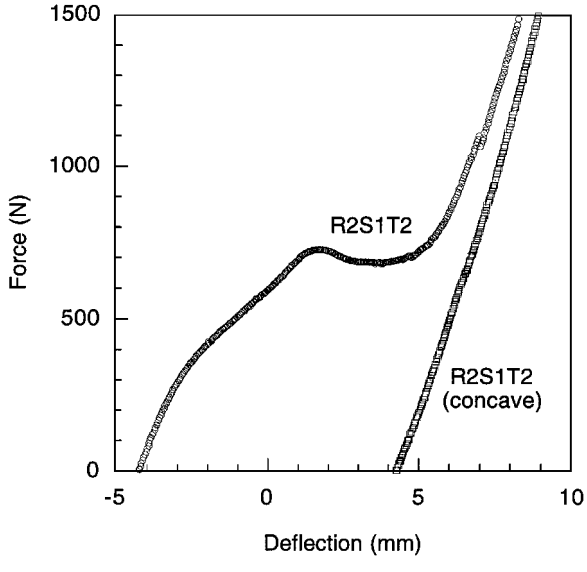

Fig. 9 Quasi-static force-deflection response with shifted deflection origin for specimen types $R_2S_1T_2$ and $R_2S_1T_2$ (concave).

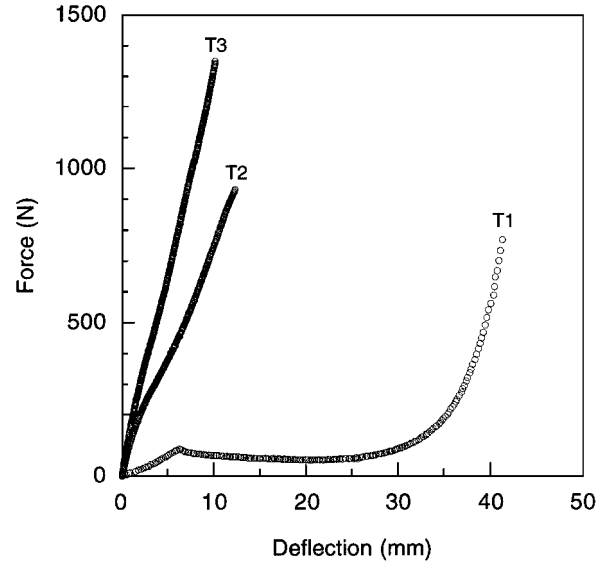

Fig. 10 Quasi-static loading response of R_3S_3 convex specimens of various thicknesses.

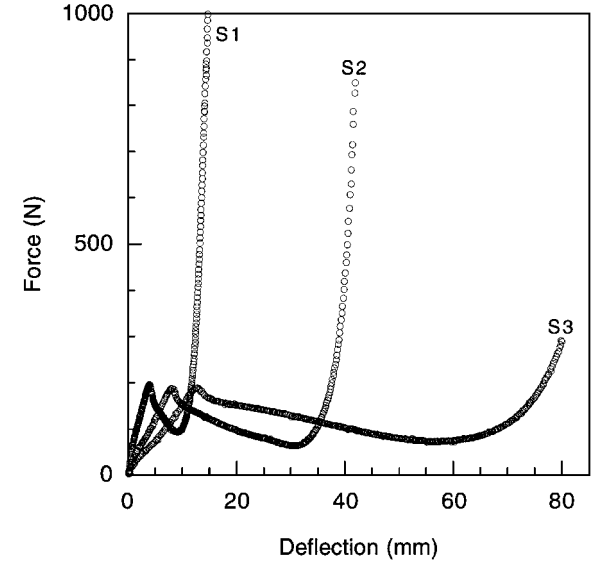

Fig. 11 Quasi-static loading response of R_2T_1 convex specimens of various spans.

and secant stiffness over the entire range of loading. Thus, characterization of the initial stiffness of the convex shell structure tells little of the specimen response after the shell transitions through the instability.

Such structural response trends, particularly with regard to specimen stiffness, can be linked to the effect of changing the radius of curvature on the mix (or ratio) of bending and membrane stiffness(es) and their contributions to the overall response. Different combinations of structural parameters can result in dominance of either the membrane or bending stiffness at different stages of the response, particularly when considering membrane stiffening. The dominant effect of membrane stiffness for some convex shells on the second equilibrium path, particularly the thinnest in the test matrix (T_1), can be considered by plotting the response for a convex and concave shell with the same structural characteristics using a translated deflection origin. The deflection origin for this comparison lies in the initial plane of a plate. A convex shell that acts primarily as a membrane, i.e., small relative bending stiffness, with this origin shift would have a loading response, after the instability, identical to a concave shell with the same structural parameters. This origin shift is performed in Fig. 8 for specimen $R_3S_1T_1$ (convex and concave) where it can be seen that the response on the second equilibrium path for the convex shell is nearly the same as that of the concave shell. However, there is a discernible difference noted in the behavior for thicker specimens as can be seen in Fig. 9 for specimens $R_2S_1T_2$ and $R_2S_1T_2$ (concave). Although the specimens appear to be approaching similar behavior, the greater bending stiffness for these thicker specimens keeps the convex shell from completely taking on the shape, and thus the behavior, of the concave shell, at least until much higher loads are reached.

Of the three structural parameters, specimen thickness has the most direct effect on both the bending and the membrane contributions to the stiffness of the laminates. As increasing specimen thickness increases both the bending and membrane stiffness, thickness should strongly affect both the initial and overall (secant) response of the structures. This can be seen in the loading response of the three convex shell specimens presented in Fig. 10, where the initial and overall stiffnesses increase with increasing thickness. This is true for all specimens tested, including plates and concave shells. Increasing the thickness generally increases the critical snapping load or eliminates it from the response as can be seen for the T_2 and T_3 specimens in Fig. 10. This is likely due to the increased bending stiffness of the laminate.

In contrast to thickness, span is noted to have little effect on the critical snapping load. This can be seen in the response curves presented in Fig. 11, which show the effect of changing the span

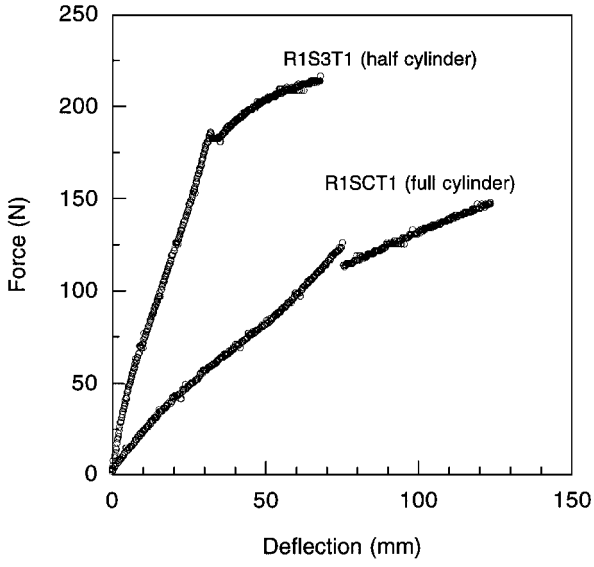

Fig. 12 Quasi-static loading respone of specimens $R_1S_3T_1$ (half-cylinder) and $R_1S_CT_1$ (full cylinder).

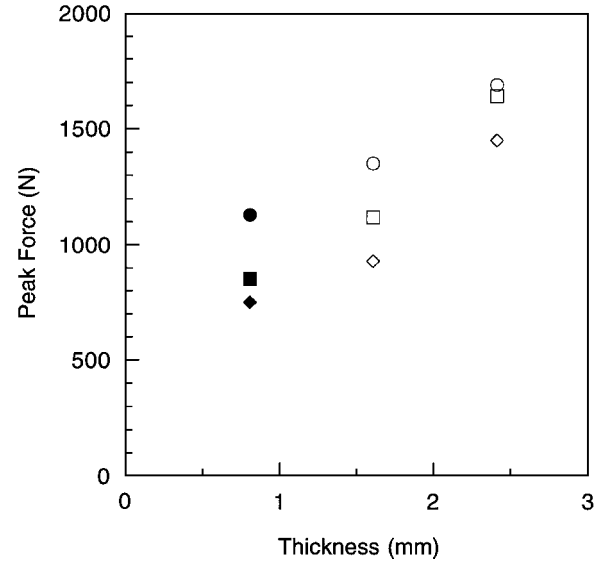

Fig. 13 Peak impact force vs thickness for various convex specimens impacted at 3 m/s (note: filled data point indicates peak force occurs on the second equilibrium path): ∘, R_1S_1; □, R_2S_2; and ◇, R_3S_3.

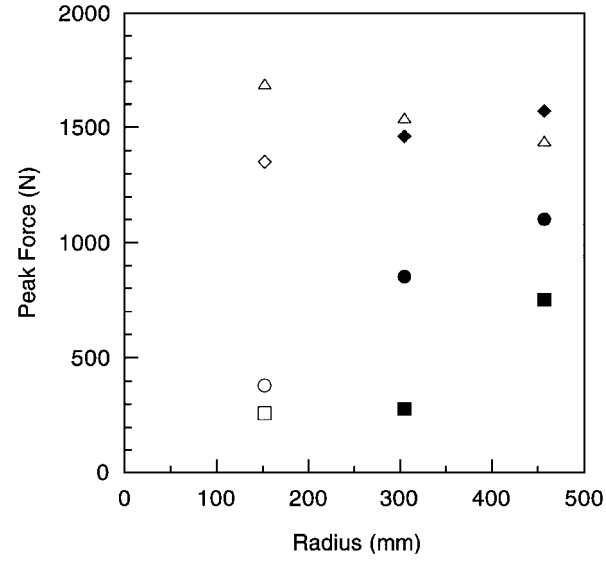

Fig. 14 Peak impact force vs radius for various convex specimens impacted at 3 m/s (note: filled data point indicates peak force occurs on the second equilibrium path): ∘, S_2T_1; ◇, S_1T_2; □, S_3T_1; and △ S_1T_3.

on the load-deflection response for convex shells with an instability. However, the effect of span on the initial specimen stiffness is clearly evident. Both the initial and overall (on the second equilibrium path) stiffnesses decrease as span is increased. These trends in stiffness are generally observed for all cases.

Although the effect of boundary conditions was not explicitly addressed for all configurations, results from the full cylinder configuration can be used to reinforce some of the other results with regard to overall load-deflection response. The full cylinder configuration tested herein is a special case of the convex shells and can be directly compared with the half-cylinder restrained in the test fixture. The cylinder response is clearly less stiff than the half-cylinder as can be seen in Fig. 12. The decreased stiffness of the full cylinder is attributed to the inextensional/flexural mode of deformation[27] in which the diameter of the cylinder elongates perpendicular to the loading. This mode of deformation is suppressed in the case of the half-cylinder by the test fixture. The absence of this boundary condition affects the mix of bending vs membrane stiffness in the two structures. With the constraint of the test fixture, the half-cylinder will have greater membrane stiffening than the unrestrained full cylinder. For a typical aircraft fuselage, the inextensional/flexural mode would also be suppressed during a small object impact, and therefore the use of full cylinders to study the impact/transverse loading response of composite shells as in, e.g., Refs. 11 and 28, should be limited to cases where this mode is likely to contribute.

The second response characteristic to consider is the peak force. Once again, the strongest effect is with thickness, which is again attributable to the overall stiffer response of thicker specimens. The trend of increasing peak force with increasing thickness can be seen in Fig. 13 where the peak force for convex specimens impacted at 3 m/s is shown. Peak force is noted to increase with increasing specimen thickness for all specimens (and configurations) tested, regardless of the instability. However, it is important to note that the peak force trend with radius changes depending on which equilibrium path the peak force occurs. This can be seen Fig. 14, where the resulting peak force for various convex specimens impacted at 3 m/s is presented. If the loading remains on the first equilibrium path, the peak force decreases with increasing radius, whereas the opposite is true if the loading reaches the magnitude of the critical snapping load on the second equilibrium path. This is likely due to the different relative roles of bending and membrane stiffness in these two regimes. Although distinct effects of span on the resulting peak force are difficult to identify, the majority of the data indicates that peak force generally decreases with increasing span regardless of the instability. As an alternative to considering the effects of individual structural parameters on the resulting peak force, nondimensional ratios of these (e.g., R/T) can be considered as well as nondimensional ratios using shell height. Shell height often appears in arch analyses, particularly as the nondimensional height-to-thickness ratio. Although the height-to-thickness ratio appears to correlate peak force over a limited range, no conclusive trends with this or any other nondimensional structural ratio were found.

Damage Resistance

The importance of peak force in correlating damage extent between impact and quasi-static tests has been discussed at the beginning of this section. The fact that peak force is a controlling parameter in damage formation is reinforced in Fig. 15, where average damage extent is plotted vs peak impact force for all specimens tested (impact and quasi-static results). The average damage extent is noted to be an increasing function of peak impact force and to increase nearly linearly for convex shells up to a force of approximately 1500 N, regardless of the structural parameters that govern the response (and, thus, peak force). Plates and concave shells are noted to also follow a nearly linear trend in Fig. 15 over the entire range of resulting peak forces. However, at peak forces above approximately 1500 N, the average damage extent increases significantly for convex shells that remain on the first equilibrium path. These specimens displayed increased damage extent as well as

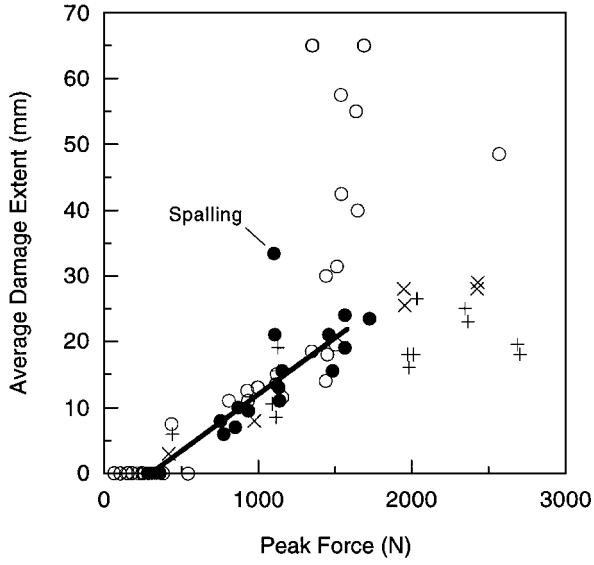

Fig. 15 Average damage extent vs peak force for plates, concave and convex shells impacted and tested quasi-statically (note: filled data point indicates peak force occurs on the second equilibrium path): ∘, convex; +, concave; and ×, plate.

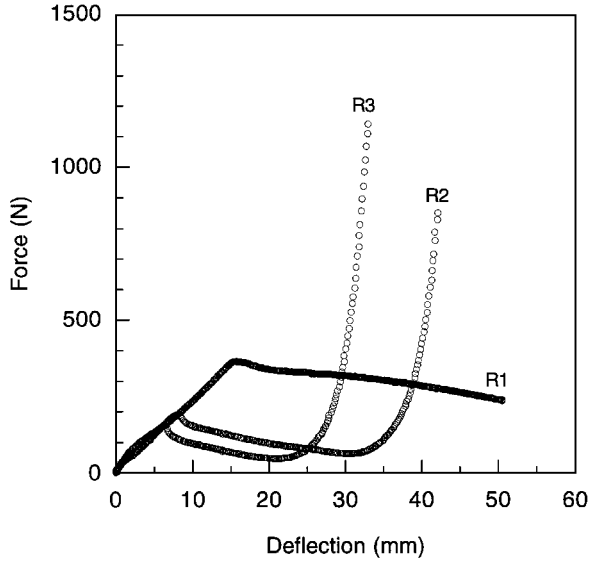

Fig. 16 Quasi-static loading response of S_2T_1 convex specimens of various radii.

atypical damage distributions. It has been hypothesized that compressive membrane stresses in convex shells that are generated when the peak force occurs on the first equilibrium path are likely a key mechanism in this type of damage formation.[29] These specimens damage to a greater extent than other convex shells with an instability (tensile membrane stresses) at an equivalent peak force. In all cases, however, damage extent is noted to increase with increasing peak force for the same laminate. Thus, increased peak force results in increased damage, with the caveat that the equilibrium path on which the peak force occurs must also be considered.

Effects of structural parameters on the resulting damage resistance should therefore be able to be evaluated by considering their effect on the resulting peak force. Thus, given a laminate and a damaging event, e.g., impact, varying structural parameters (radius and span in this investigation) such that peak force increases should produce increased damage. The quasi-static response curves shown in Fig. 16 show that as the radii of these shells increases, the peak force also increases. These curves are related to the impact response of the same specimens through the peak force metric, i.e., the specimens in Fig. 16 are loaded to the same peak force as that measured in the impact tests at 3 m/s. The x radiographs of the damage states for these specimens are shown in Fig. 17 and have average damage

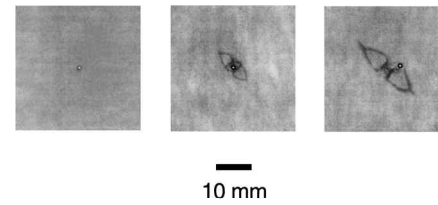

Fig. 17 Damage *x* radiographs for S_2T_1 convex specimens (quasi-static loading response in Fig. 17): $R_1S_2T_1$ (on the left), $R_2S_2T_1$ (in the center), and $R_3S_2T_1$ (on the right).

extents of 0 (no damage), 7, and 11 mm with increasing radius, respectively. Damage becomes more severe at higher radii due to the higher peak force during the loading event. Thus, the effect of varying a structural parameter can be evaluated by considering the effect on the structural response and, in particular, the resulting peak force. This trend holds for other cases in this investigation as well. However, attention must also be given to structural parameters that cause the peak force to remain on the first equilibrium path as damage extent increases significantly (and is of a different nature) for convex shells. Structural parameters that cause the peak force to remain on the first equilibrium path, effectively delaying the onset of the instability, include increased curvature (decreased radius) and increased thickness.

The trend of impact damage with regard to varying structural parameters has been explained through the peak force attained during the loading. A key mechanism by which the structural parameters affect the peak force, and thus damage, is through the development of the instability region. During an impact event, the energy of the impactor must be absorbed by the specimen through structural deformation and damage. Specimens that can absorb greater amounts of impact energy without reaching high peak forces will be more damage resistant. As always, the equilibrium path must also be considered. For example, it has previously been shown that convex shells can be more damage resistant than corresponding plate specimens due to the instability.[29] The convex shells absorb the impact energy through large deformations through the instability region, whereas the plate, having no instability, loads monotonically to high peak forces to absorb the impact energy. Thus, the plate is damaged to a greater extent than the shell for a given impact event. The trend with radius for convex shells established herein further substantiates this finding. Shells with more curvature have larger instability regions and reach lower peak forces as in Fig. 16. Likewise, increasing the span has the same effect on the instability region and the resulting damage.

The effect that structural parameters have on the instability region of convex shells is therefore particularly important in evaluating damage resistance. The energy absorbed (elastically) through the instability region is proportional to the critical snapping load and the deflections associated with the instability region. This elastic deformation, which is not associated with increasing the peak load beyond the critical snapping load, effectively improves impact damage resistance. Utilizing the finding that no specimens damage below a (threshold) peak force of approximately 400 N, structural parameters that result in critical snapping loads below 400 N will contribute to the impact damage resistance of these specimens. For example, specimen $R_1S_2T_1$ approaches 400 N in Fig. 16 and undergoes extremely large deformations (over 60 times the specimen thickness) through the instability region, but the specimen is not damaged. It is logical then to conclude that if the critical snapping load is below the damage incipience threshold, a convex specimen will not damage until the loading (e.g., impact) event is severe enough to push the response to higher peak forces on the second equilibrium path. Thus, structural parameters that can maximize energy consumption through the instability region, with critical snapping loads below the incipient threshold, will be most damage resistant.

Summary

The transverse loading response of various composite shell structures was investigated experimentally. Quasi-static and impact tests at different velocities were used to evaluate the structural response

(including damage). Basic structural parameters (radius, span, and thickness) were independently varied to determine their effects on the resulting response. Load-deflection curves, peak force, and instability parameters such as the critical snapping load are used to characterize the effect of the structural parameters on the response.

The results of this work establish trends with regard to structural parameters (radius, span, and thickness) and general response characteristics of composite shells under transverse loading. Given the peak force damage resistance metric, these results have application to low-velocity impact due to the equivalence demonstrated previously between impact and quasi-static tests. Variations in the structural parameters are noted to affect the initial and overall (secant) specimen stiffness, the critical snapping load, the deflections associated with the instability, and damage resistance. Of the three structural parameters, thickness is noted to have the greatest effect on the loading response and resulting peak force. This is attributed to the increased laminate membrane and bending stiffnesses as thickness increases. Shell radius is also clearly important due to the (dominant) effects of the instability in convex shell response. For example, the trend of peak force with radius is noted to reverse depending upon which equilibrium path the response ends.

Damage resistance is related to variations in the structural parameters through their effect on the peak force attained during the loading event. Due to the impact energy consumption mechanism of structural deformation through the instability region, decreasing radius, increasing span, and decreasing thickness are generally shown to enhance impact damage resistance for convex shells. However, when the convex shell response remains on the first equilibrium path, damage resistance of the composite shells is detrimentally affected. This is attributed to compressive membrane stresses that promote sublaminate buckling, and thus delamination growth, on the first equilibrium path.

It should be noted that the loading response plots presented in this work represent an average specimen response, i.e., information such as deflection mode shapes is not known. Furthermore, a determination of whether the critical snapping load is associated with bifurcation or limit point buckling cannot be made from the force-deflection data. The data also necessarily contain the effects of specimen imperfections (imperfection sensitivity), loading misalignments (however slight), unsymmetric and mathematically imperfect boundary conditions, and other such effects. Boundary conditions are known to be important in a general sense and specifically in the response of thin composite shells,[30,31] particularly when shell instabilities are involved.[32] Imperfections, whether in the form of loading misalignments or manufacturing defects, likewise can alter the resulting response. The effects of boundary conditions, imperfections, and the possibility of unsymmetric deformation modes on the impact damage resistance of composite shells are recommended areas of future study.

Contributions to the damage state from both membrane and bending stresses, particularly for shells that were shown to damage severely on the first equilibrium path, should likewise be further investigated. Modeling of composite shells to determine the effects of both structural parameters and the instability region on the resulting damage state are required to fully understand mechanisms (such as membrane stresses and energy-consuming ability) that affect damage resistance. Analytical and numerical parametric studies should be undertaken to evaluate the relative importance of each structural parameter on the resulting shell response. Only by investigating the relative importance of these many effects can we attain the needed more general understanding of the response of composite shells to transverse loading.

Acknowledgments

This work was sponsored by the Federal Aviation Administration under Research Grant 94-G-037 and the NASA Langley Research Center under NASA Grant NAG-1-991.

References

[1]Amatore, D., "Composite Hydrogen Tank Test Completed for DC-XA," Marshall Space Flight Center, NASA News Press Release 96-13, Huntsville, AL, Jan. 1996.

[2]Breivik, N. L., Gurdal, Z., and Griffin, O. H., "Compression of Laminated Composite Beams with Initial Damage," *Proceedings of the American Society for Composites 7th Technical Conference*, Technomic, Lancaster, PA, 1992, pp. 972–981.

[3]Chen, G.-S., Bidinger, G. M., and Lou, M. C., "Impact Damage in Small Diameter Graphite/Epoxy Composite Struts," *Proceedings of the AIAA/ASME/ASCE/AHS 33rd Structures, Structural Dynamics, and Materials Conference*, AIAA, Washington, DC, 1992, pp. 2945–2954.

[4]Abrate, S., "Impact on Laminated Composites: Recent Advances," *Applied Mechanics Review*, Vol. 47, No. 11, 1994, pp. 517–544.

[5]Abrate, S., "Impact on Laminated Composite Materials," *Applied Mechanics Review*, Vol. 44, No. 4, 1991, pp. 155–190.

[6]Cantwell, W. J., and Morton, J., "The Impact Resistance of Composite Materials," *Composites*, Vol. 22, No. 5, 1991, pp. 55–97.

[7]Palazotto, A. N., Chien, L. S., and Taylor, W. W., "Stability Characteristics of Laminated Cylindrical Panels Under Transverse Loading," *AIAA Journal*, Vol. 30, No. 6, 1992, pp. 1649–1653.

[8]Kim, D., and Chaudhuri, R. A., "Full and Von Kármán Geometrically Nonlinear Analyses of Laminated Cylindrical Panels," *AIAA Journal*, Vol. 33, No. 11, 1995, pp. 2173–2181.

[9]Chang, T. Y., and Sawamiphakdi, K., "Large Deformation Analysis of Laminated Shells by Finite Element Method," *Computers and Structures*, Vol. 13, No. 1, 1981, pp. 331–340.

[10]Tsai, C. T., Palazotto, A. N., and Dennis, S. T., "Large-Rotation Snap-Through Buckling in Laminated Cylindrical Panels," *Finite Elements in Analysis and Design*, Vol. 9, No. 1, 1991, pp. 65–75.

[11]Chang, F.-K., and Kutlu, Z., "Strength and Response of Cylindrical Composite Shells Subjected to Out-of-Plane Loadings," *Journal of Composite Materials*, Vol. 23, Jan. 1989, pp. 11–31.

[12]Johnson, E. R., Hyer, M. W., and Carper, D. M., "Response of Composite Material Shallow Arch to Concentrated Load," *Proceedings of the AIAA/ASME/ASCE/AHS 25th Structures, Structural Dynamics, and Materials Conference*, AIAA, New York, 1984, pp. 310–321.

[13]Lagace, P. A., and Wolf, E., "Impact Damage Resistance of Several Laminated Material Systems," *AIAA Journal*, Vol. 33, No. 6, 1995, pp. 1106–1113.

[14]Niu, M. C. Y., *Airframe Structural Design—Practical Design Information and Data on Aircraft Structures*, 8th ed., Conmilit Press Ltd., Los Angeles, CA, 1995, pp. 384–389.

[15]Jackson, W. C., and Poe, C. C., Jr., "The Use of Impact Force as a Scale Parameter for the Impact Response of Composite Laminates," *Journal of Composites Technology & Research*, Vol. 15, No. 4, 1992, pp. 282–289.

[16]Lagace, P. A., Williamson, J. E., Tsang, P. H. W., Wolf, E., and Thomas, S., "A Preliminary Proposition for a Test Method to Measure (Impact) Damage Resistance," *Journal of Reinforced Plastics and Composites*, Vol. 12, No. 5, 1993, pp. 584–601.

[17]Wardle, B. L., "Impact and quasi-static Response of Cylindrical Composite Shells," Technology Lab. for Advanced Composites, TELAC Rept. 95-4, Massachusetts Inst. of Technology, Cambridge, MA, May 1995.

[18]Lagace, P. A., Brewer, J. C., and Varnerin, C., "TELAC Manufacturing Course Notes," Technology Lab. for Advanced Composites, TELAC Rept. 88-4B, Massachusetts Inst. of Technology, Cambridge, MA, May 1988.

[19]Lie, S. C., "Damage Resistance and Damage Tolerance of Thin Composite Facesheet Honeycomb Panels," Technology Lab. for Advanced Composites, TELAC Rept. 89-3, Massachusetts Inst. of Technology, Cambridge, MA, March 1989.

[20]Ryan, K. F., "Dynamic Response of Graphite/Epoxy Plates Subjected to Impact Loading," Technology Lab. for Advanced Composites, TELAC Rept. 89-13, Massachusetts Inst. of Technology, Cambridge, MA, Sept. 1989.

[21]Freeman, S. M., "Characterization of Lamina and Interlaminar Damage in Graphite/Epoxy Composites by the Deply Technique," *Composite Materials: Testing and Design*, ASTM STP 787, American Society of Testing and Materials, Philadelphia, PA, 1982, pp. 50–62.

[22]Chang, F. H., Couchman, J. C., Eisenmann, J. R., and Lee, B. G. W., "Application of a Special X-Ray Nondestructive Testing Technique for Monitoring Damage Zone Growth in Composite Laminates," *Composite Reliability*, ASTM STP 580, American Society of Testing and Materials, Philadelphia, PA, 1975, pp. 176–190.

[23]Wu, H. Y.-T., and Springer, G. S., "Measurements of Matrix Cracking and Delamination Caused by Impact on Composite Plates," *Journal of Composite Materials*, Vol. 22, June 1988, pp. 518–532.

[24]Bazant, Z. P., and Cedolin, L., *Stability of Structures: Elastic, Inelastic, Fracture, and Damage Theories*, Oxford Engineering Science Series, Oxford Univ. Press, New York, 1991, pp. 108–118.

[25]Marshall, I. H., and Rhodes, J., "Snap-Buckling of Thin Shells of Rectangular Planform," *Stability Problems in Engineering Structures and Components*, edited by T. H. Richards and P. Stanley, Applied Science, London, 1979, pp. 249–264.

[26]Wardle, B. L., and Lagace, P. A., "On the Use of quasi-static Testing to Assess Impact Damage Resistance of Composite Shells," *Mechanics of Composite Materials and Structures,* Vol. 5, No. 1, 1998, pp. 1–19.

[27]Timoshenko, S., and Woinowsky-Krieger, S., *Theory of Plates and Shells*, 2nd ed., McGraw–Hill, New York, 1959, pp. 501–507.

[28]Christoforou, A. P., and Swanson, S. R., "Analysis of Simply Supported Orthotropic Cylindrical Shells Subject to Lateral Impact Loads," *Advanced Composites and Processing Technology: Presented at the Winter Annual Meeting of the American Society of Mechanical Engineers*, edited by T. H. Tsiang and R. N. Taylor, American Society of Mechanical Engineers, New York, 1988, pp. 77–84.

[29]Wardle, B. L., and Lagace, P. A., "Importance of Instability in Impact Response and Damage Resistance of Composite Shells," *AIAA Journal*, Vol. 35, No. 2, 1997, pp. 389–396.

[30]Marshall, I. H., Rhodes, J., and Banks, W. M., "The Nonlinear Behaviour of Thin, Orthotropic, Curved Panels Under Lateral Loading," *Journal of Mechanical Engineering Science*, Vol. 19, No. 1, 1977, pp. 30–37.

[31]Tudela, M. A., "Structural Response and Damage Development of Cylindrical Composite Panels," Technology Lab. for Advanced Composites, TELAC Rept. 96-11, Massachusetts Inst. of Technology, Cambridge, MA, Sept. 1996.

[32]Arbocz, J., and Hoi, J. M. A. M., "The Role of Experiments in Improving the Computational Models for Composite Shells," *Analytical and Computational Models of Shells*, edited by A. K. Noor, T. Belytschko, and J. C. Simo, American Society of Mechanical Engineers, New York, 1989, pp. 613–640.

A. M. Waas
Associate Editor